Acta Crystallographica Section D
Biological Crystallography
ISSN 0907-4449

Structure of *Pseudomonas aeruginosa* Hfq protein

Alexey Nikulin,[a]* Elena Stolboushkina,[a] Anna Perederina,[a,b] Ioulia Vassilieva,[a] Udo Blaesi,[c] Isabella Moll,[c] Galina Kachalova,[d] Shigeyuki Yokoyama,[b,e,f,g] Dmitry Vassylyev,[b,e] Maria Garber[a] and Stanislav Nikonov[a]

[a]Institute of Protein Research, Russian Academy of Sciences, 142290 Pushchino, Moscow Region, Russia, [b]Structural and Molecular Biology Laboratory, RIKEN Harima Institute at SPring-8, 1-1-1 Kouto, Mikazuki-cho, Sayo, Hyogo 679-5148, Japan, [c]Max Perutz Laboratories, Institute of Microbiology and Genetics, University Departments at the Vienna Biocenter, Austria, [d]Max Planck Unit for Structural Molecular Biology, DESY, Hamburg, Germany, [e]Structurome Research Group, RIKEN Harima Institute at SPring-8, 1-1-1 Kouto, Mikazuki-cho, Sayo, Hyogo 679-5148, Japan, [f]RIKEN Genomic Sciences Center, 1-7-22 Suehiro-cho, Tsurumi, Yokohama 230-0045, Japan, and [g]Department of Biophysics and Biochemistry, Graduate School of Science, University of Tokyo, 7-3-1 Hongo, Bunkyo-ku, Tokyo 113-0033, Japan

Correspondence e-mail: nikulin@vega.protres.ru

Received 9 September 2004
Accepted 18 November 2004

PDB References: Hfq protein, 1u1s, r1u1ssf; 1u1t, r1u1tsf.

The structure of the Hfq protein from *Pseudomonas aeruginosa* was determined using two different ionic conditions. In both cases the molecules formed identical hexameric rings, but some variations in the crystal packing were revealed. Hfq belongs to the family of Sm/LSm proteins, the members of which can form hexameric as well as heptameric rings. Comparative analysis of known structures of this protein family shows that the fragment of the Sm-fold responsible for oligomerization is strongly structurally conserved. In the heptameric ring, three conserved hydrogen bonds between β-strands of adjacent molecules hold together the monomers, whereas in the hexameric rings of Hfq an additional conserved inaccessible hydrogen bond between neighbouring monomers is observed.

1. Introduction

Hfq is an abundant RNA-binding bacterial protein that was first identified as a host factor required for plus-strand replication of the Qβ RNA bacteriophage (Franze de Fernandez *et al.*, 1972). In bacterial cells, Hfq appears to function as a global regulator of gene expression. Hfq has been reported to be a bacterial Sm-like protein that mediates RNA–RNA interactions (Zhang *et al.*, 2002; Møller *et al.*, 2002). Synthesis of more than 30 proteins is affected in an *Escherichia coli hfq*$^-$ mutant (Muffler *et al.*, 1997) including proteins of DNA-repair pathways (Tsui *et al.*, 1997), proteins involved in iron metabolism (Večerek *et al.*, 2003) as well as the synthesis of the σ^S subunit of RNA polymerase and consequently all σ^S-dependent genes (Muffler *et al.*, 1997). Hfq is believed to stimulate *rpoS* translation by mediating binding of the small RNAs (sRNAs) DsrA and RprA to their complementary target sequence in the 5′ untranslated region of *rpoS* mRNA, thereby allowing ribosome binding (Sledjeski *et al.*, 2001; Majdalani *et al.*, 2002). In *Pseudomonas aeruginosa*, Hfq (PaeHfq) is involved in regulation of virulence-factor synthesis (Sonnleitner *et al.*, 2003).

Hfq is a small (8–11 kDa) thermostable protein that exists in a hexameric form in solution (Kajitani *et al.*, 1994). The sequence of its core part is highly conserved, whereas the C-terminal tail varies in length in different bacteria and its function remains unknown. *E. coli* Hfq (EcoHfq) has a much longer C-terminal tail than PaeHfq. Nevertheless, PaeHfq has been shown to functionally replace EcoHfq in terms of its requirement for phage Qβ replication and for *rpoS* expression (Sonnleitner *et al.*, 2002). The crystal structures of *Staphylococcus aureus* Hfq (SauHfq) and of a truncated form of EcoHfq have recently been determined (Schumacher *et al.*, 2002; Sauter *et al.*, 2003). This work describes the structure of full-length PaeHfq determined at 1.6 Å resolution under two different ionic environments.

Table 1
Crystal properties and diffraction data statistics.

Values in parentheses are for the highest resolution shell.

	Crystal *A*	Crystal *B*
Crystallization conditions	1 *M* Li_2SO_4, 0.6 *M* $(NH_4)_2SO_4$, 100 m*M* MES pH 6.5, 5 m*M* $CdCl_2$	200 m*M* NH_4Cl, 12% PEG 4000, 50 m*M* Tris–HCl pH 8.5, 5 m*M* $CdCl_2$
Space group	$P2_12_12_1$	$P2_12_12_1$
Unit-cell parameters (Å)	a = 61.18, b = 73.37, c = 106.04	a = 61.44, b = 72.35, c = 109.25
Resolution (Å)	15–1.6 (1.7–1.6)	25–1.9 (2.0–1.9)
Completeness (%)	97.1 (93.8)	97.8 (96.5)
$I/\sigma(I)$	15.9 (4.1)	12.9 (3.9)
Redundancy	3.9 (3.7)	10.2 (4.7)
R_{merge} (%)	4.2 (32.5)	8.4 (28.4)

2. Materials and methods

2.1. Gene cloning and expression

The *hfq* gene from *P. aeruginosa* was cloned into pET22b(+) expression vector. *Nde*I and *Bam*HI restriction sites were used and *E. coli* DH5α strain was transformed using the resulting plasmid. After PCR screening, the plasmid with correct-sized insert was checked by direct sequencing. *E. coli* strain BL21(DE3)/pUBS520 was transformed using the recombinant plasmid and plated on LB agar with 100 µg ml^{-1} ampicillin. 3 ml LB media containing the antibiotic were infected with several colonies and the culture was grown overnight at 310 K. This overnight culture was added to 1 l LB media containing 100 µg ml^{-1} ampicillin and incubated in a shaker (160 rev min^{-1}) at 310 K until OD_{590} reached 0.6. At this point, protein production was induced using 1 m*M* isopropyl-β-D-thiogalactopyranoside and the cells were harvested by centrifugation (8000 rev min^{-1}, Beckman JA-10 rotor, 277 K, 10 min) after 3 h incubation.

2.2. Protein purification

4 g of wet cells were suspended in 20 ml 50 m*M* Tris–HCl pH 8.0, 250 m*M* $MgCl_2$, 1 *M* NaCl, 5 m*M* EDTA and disintegrated by sonication. Cellular membranes were removed by centrifugation for 20 min at 14 000*g*. Proteins from the host strain were removed by heating at 358 K for 20 min and subsequent centrifugation for 40 min at 14 000*g*. Ammonium sulfate was added to the supernatant to 1.7 *M* final concentration and loaded onto a Butyl-Toyopearl column. After washing the column with a solution containing 1.5 *M* ammonium sulfate and 1 *M* NaCl, the protein was eluted with a linear gradient of 1.5–0 *M* ammonium sulfate and 1–0.1 *M* NaCl in 50 m*M* Tris–HCl pH 8.0. The fractions that were homogeneous by UV spectral and Coomassie blue-stained SDS–PAGE analysis were pooled and concentrated. The protein was then diluted with 50 m*M* Tris–HCl pH 8.0, 100 m*M* NaCl buffer and loaded onto a DEAE-Sepharose column. The protein flowing through the column was concentrated to 30–12 mg ml^{-1}.

Table 2
Refinement statistics.

Values in parentheses are for the highest resolution shell.

	Crystal *A*	Crystal *B*
No. of non-H protein atoms	3184	3216
No. of solvent atoms	243	164
Resolution range	15–1.6 (1.7–1.6)	25–1.9 (2.0–1.9)
No. of reflections	61217 (9712)	38033 (5817)
R (%)	22.3 (33.9)	20.5 (32.9)
R_{free} (%)	25.0 (36.9)	25.3 (36.5)
Mean temperature factor B (Å^2)	28.9	35.4
Main chain	26.5	31.9
Side chain	31.3	38.9
Solvent	40.4	39.4
R.m.s. deviation from ideal values		
Bond lengths (Å)	0.006	0.006
Bond angles (°)	1.3	1.2
Dihedral angles (°)	25.0	23.9
Improper angles (°)	0.95	0.86
Ramachandran plot		
Most favoured	319 (92.2%)	316 (90.5%)
Additionally allowed	21 (6.1%)	28 (8.0%)
Generously allowed	6 (1.8%)	5 (1.5%)
Rm.s.d. (Å) between monomers C^α/all atoms		
A/*B*	0.52/0.99	0.54/1.08
A/*C*	0.67/1.20	0.62/1.21
A/*D*	0.40/0.82	0.37/0.77
A/*E*	0.64/1.13	0.86/1.30
A/*F*	0.64/1.25	0.67/1.26

2.3. Crystallization and data collection

Crystals of PaeHfq were obtained by the hanging-drop vapour-diffusion technique at 295 K. All drops were set up by mixing 2.0 µl protein, dialyzed into 20 m*M* Tris–HCl pH 8.0, 200 m*M* NaCl, 200 m*M* ammonium sulfate, with 2.0 µl precipitant solution on siliconized cover slides and were equilibrated against 1.0 ml of the same precipitant solution. PaeHfq formed crystals with two different precipitant solutions: (i) 1 *M* Li_2SO_4, 0.6 *M* ammonium sulfate, 100 m*M* MES pH 6.5 and (ii) 200 m*M* NH_4Cl, 12% PEG 4000, 50 m*M* Tris–HCl pH 8.5 (referred to in subsequent discussion as crystal *A* and crystal *B*). In both cases $CdCl_2$ was used as an additive at a final concentration of 5 m*M* and large single crystals were obtained. Before freezing in liquid nitrogen, the crystals were transferred to 15% ethylene glycol, 2 *M* $Li_2SO_4{\cdot}H_2O$, 100 m*M* MES pH 6.5, 10 m*M* $CdCl_2$ for crystal *A* and 15% PEG 3350, 15% PEG 400, 200 m*M* NH_4Cl, 50 m*M* Tris–HCl pH 8.5 for crystal *B*.

X-ray diffraction data from crystal *A* were collected at the MPG/GBF beamline BW6 at DESY (Hamburg, Germany) using a MAR CCD detector and processed using the *XDS* program (Kabsch, 1993). Data from crystal *B* were collected at SPring-8 (Harima, Japan) using an R-AXIS V image-plate detector and processed using the *HKL*2000 program package (Otwinowski & Minor, 1997). Detailed data-collection statistics are shown in Table 1.

2.4. Determination and refinement of the structures

The *AMoRe* program package (Navaza, 1994) was used to solve the structures by the molecular-replacement method. A hexamer of EcoHfq (PDB code 1hk9) with appropriate

changes in the sequence was used as a model for both crystal forms. For diffraction data between 15 and 3.0 Å, the model gave clear solutions with a correlation coefficient of 46.9 and an R factor of 48.8% for crystal A and with a correlation coefficient of 75.5 and R factor of 33.3% for crystal B. Both structures were subjected to several rounds of computational refinement and map calculation with *CNS* (Brünger *et al.*, 1998) and manual model inspection and modification with *O* (Jones *et al.*, 1991). A free R factor calculated from 5% of reflections set aside at the outset was used to monitor the progress of refinement. The initial anisotropic overall B factor was replaced successively with per-residue B factors, separate per-residue B factors for main-chain and side-chain atoms and, finally, restrained individual atomic B factors. The model bias present in the initial molecular-replacement solutions was tackled using composite omit cross-validated σ_A-weighted maps implemented in *CNS*. When the R-factor value reached 30%, water molecules were placed into 3σ peaks in $F_o - F_c$ maps when they were within a suitable hydrogen-bonding distance of the existing model. After refinement, water molecules whose positions were not supported by the electron density at 1σ contouring in a σ_A-weighted $2F_o - F_c$ map were deleted. The final models for crystals A and B, refined to 1.6 and 1.9 Å, respectively, incorporate 3184 and 3216 non-H atoms (Table 2). The electron-density map was of sufficient quality (Fig. 1) to trace the polypeptide chains, including residues 5–71.

3. Results and discussion

3.1. Overall structure description

PaeHfq, like other known bacterial Hfq proteins, forms a symmetric doughnut-shaped homo-hexamer with a thickness of ∼26 Å and outer and inner diameters of ∼65 and 8 Å, respectively (Fig. 2*a*). Each monomer (Fig. 2*b*) contains helix α1, a universal Sm-fold and distorted N- and C-terminal tails. The Sm-fold includes two sequence motifs, Sm1 and Sm2 (Hermann *et al.*, 1995; Seraphin, 1995).

The connectivity scheme of the fragment, corresponding to the Sm1 motif, is β1, L2, β2, L3, β3 (Figs. 2*b* and 3). This motif can be represented as a V-shaped triple-stranded β-sheet formed by two β–β hairpins (Efimov, 1992), which are set at an angle of about 60° to each other. Both hairpins contain a long bent strand β2 and strands β1 and β3 contacting the N- and C-termini of β2, respectively. The Sm1 fragment is perpendicular to the plane of the hexamer and mainly constitutes its outer surface. Hydrogen bonds formed by main-chain atoms of highly conserved Gly34 (Fig. 2*c*) with the N-terminal end of β1 and the C-terminal end of β3 stabilize this structure.

The connectivity scheme of the fragment corresponding to the Sm2 motif includes strands β4 and β5 and loop L5 between them (Figs. 2*b* and 3). This motif is responsible for the contacts between monomers and can also be represented as a V-shaped structure which is approximately parallel to the plane of the hexamer and perpendicular to the Sm1 fragment. Loop L4, which connects the Sm1 and Sm2 motifs, is located on the outer side of the hexameric ring close to the C-terminal end of an adjacent monomer. There is no unambiguously interpretable electron density for this part of some monomers, especially for the structure obtained under low ionic conditions. Both fragments corresponding to the Sm1 and Sm2 motifs are embedded into each other and are incorporated in the two β-sheets.

The N- and C-termini of all monomers are very flexible. In both of the structures determined under different ionic conditions there is no interpretable electron density for residues 1–4 and 72–82. Residue His5 was found to be incorporated into helix α1. The visible part of the C-terminal tail, containing residues 66–71, is approximately antiparallel to helix α1. Both N- and C-termini are located close to each other and directed into the solvent.

3.2. The structures at two different ion conditions

The crystals containing intact PaeHfq molecules (82 amino-acid residues) obtained under two different ionic conditions (Table 1) belong to the same space group and have approximately similar unit-cell parameters. Nevertheless, they diffract to different resolutions and a comparison of the two corresponding data sets showed more than 20% difference. We proposed that this could be a result of changes in the PaeHfq conformations and solved and refined both structures separately. Nevertheless, superposition of hexamers corresponding to these structures yielded a very small r.m.s. deviation of 0.26 Å. This means that the ionic conditions do not affect the PaeHfq fold and oligomerization.

Analysis of the crystal packing of the two crystals obtained under different ionic conditions shows that the hexamers are slightly rotated and displaced relative to each other by a distance of about 1.5 Å. Consequently, differences in crystal packing account for the observed difference between the intensity data in the two native data sets.

The structure obtained at low ionic strength also exhibits a higher mobility of its main-chain atoms, especially at the N- and C-termini and in the loop L4 region. The residues of loop L4 have poor electron density in the map corresponding to the low-salt PaeHfq crystal, but can be easily traced in the map corresponding to the high-salt crystal. The B-factor plot of the main-chain atoms clearly indicates the flexibility of loop L4 as well as the N- and C- terminal tails of the protein.

3.3. Hfq C-terminal tail

The length of the C-terminal tails of Hfq from different organisms vary from nine residues in *Bacillus subtilus* to 38 in EcoHfq (Fig. 3) with no considerable homology among known sequences. The C-terminal tail of PaeHfq contains 18 residues. In all known structures of the Hfq proteins there are no coordinates for the full-length C-terminal tails. The longest part of the tail, containing seven residues, was determined for some monomers of EcoHfq (Sauter *et al.*, 2003).

PaeHfq, as well as C-terminally truncated EcoHfq lacking the last 27 amino acids, can functionally replace the EcoHfq protein *in vivo* in phage Qβ replication, *rpoS* and *ompA*

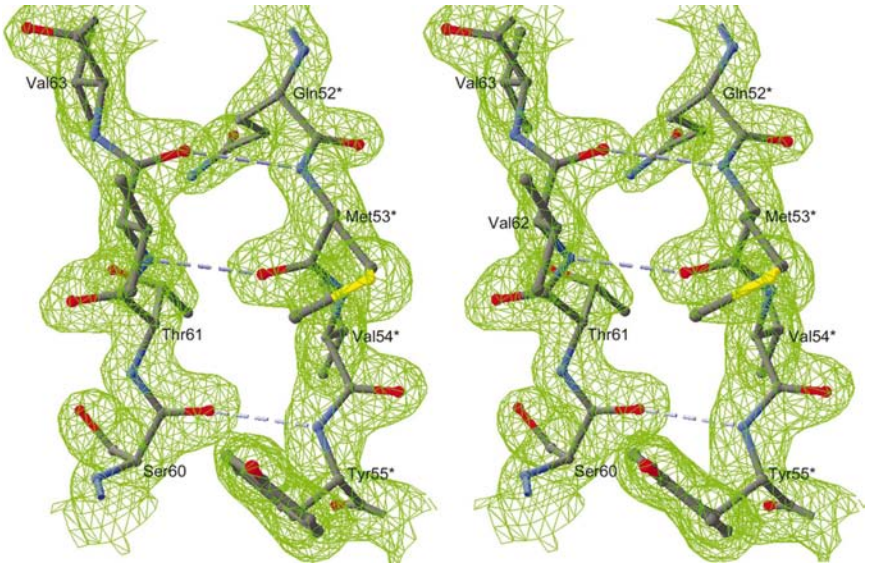

Figure 1
A fragment of the final $2F_o - F_c$ map at 1.6 Å resolution, showing the intersubunit interface. The map is contoured at the 2.5σ level. The hydrogen bonds between strands $\beta4$ and $\beta5$ of adjacent monomers are shown by dotted lines.

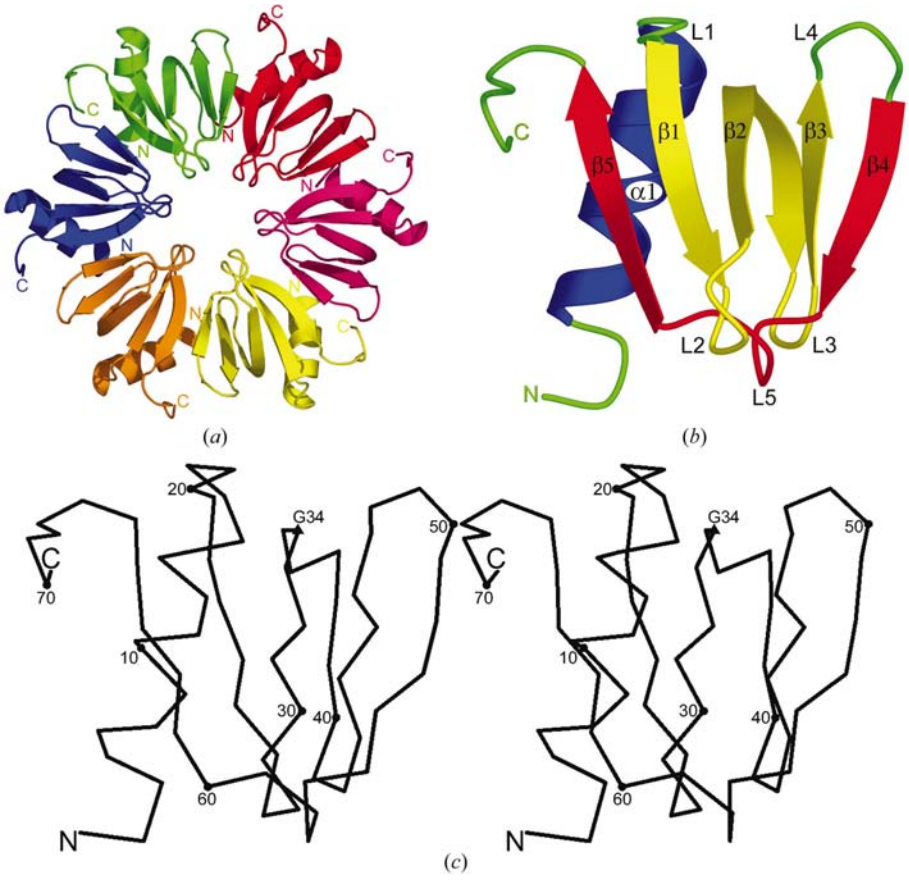

Figure 2
The structure of the Hfq protein from *P. aeruginosa*. (*a*) Top view of the Hfq hexameric ring. (*b*) Schematic representation of the Hfq monomer. The structure corresponding to the Sm1 motif is marked in yellow; the structure corresponding to the Sm2 motif is marked in red. (*c*) Stereoview of the C^{α} trace of PaeHfq. Every tenth C^{α} atom is represented by a sphere. The highly conserved Gly34 is marked by a triangle.

expression (Sonnleitner *et al.*, 2002). Likewise, truncation of the 19 C-terminal amino acids of EcoHfq did not affect the RNA-binding properties (Arluison *et al.*, 2004). Relying on such experiments, it has been proposed that the C-terminus of this protein is dispensable for its interaction with RNA. Nevertheless, full-length EcoHfq is more stable than truncated EcoHfq and electron microscopy indicates a structural rearrangement between the monomers upon truncation (Arluison *et al.*, 2004). Such rearrangements and the high contents of charged and polar residues in the C-terminal tails testify that the C-terminal extension could increase the stability of some RNA–protein complexes.

In both of the crystals of PaeHfq obtained under different ionic conditions the quality of the electron-density map decreased markedly in the C-terminal area and only allowed tracing the polypeptide chain up to Pro71. In both of our models residues 65–71 have close conformations and are located on the outer surface of the hexamers.

3.4. Oligomerization

Strand $\beta4$, loop L5 and strand $\beta5$ form the strongly conserved structural fragment corresponding to the Sm2 motif (Table 3). This fragment is responsible for the formation of hexameric as well as heptameric rings in Sm/LSm proteins. The interaction between β-strands 4 and 5 of two adjacent monomers (Fig. 4) is a common feature of all known Sm proteins and provides the formation of a continuous β-sheet in the Sm oligomers. In PaeHfq this continuous β-sheet is stabilized by three inaccessible hydrogen bonds (Met53 N–Val*62 O, Met53 O–Val*62 N and Tyr55 N–Ser*60 O) between $\beta4$ and $\beta5$ (Figs. 1 and 4). The specific and complementary distribution of the atoms forming these hydrogen bonds along strands $\beta4$ and $\beta5$ could be responsible for the correct orientation of monomers under oligomerization. Thus, in strand $\beta4$ the distance between Met53 N and Met53 O is equal to 2.8 Å, whereas the

Table 3
R.m.s.d. of the conserved structural element, responsible for oligomerization, in different Hfq and Sm-proteins.

	Eco	Pae	Sau	AF-Sm1	AF-Sm2
Eco	+	0.483	0.448	0.566	0.577
Pae		+	0.374	0.353	0.535
Sau			+	0.512	0.622
AF-Sm1				+	0.488
AF-Sm2					+

distance between Met53 O and Tyr55 N is 4.1 Å. The distances between corresponding atoms belonging to strand $\beta5$ of the adjacent monomer are 2.8 and 4.8 Å, respectively. Similar location of such hydrogen-bonded atoms has been found in all known structures of Sm-like proteins. As a result, in all ring-like Sm structures strand $\beta4$ of one monomer is antiparallel to strand $\beta5$ of an adjacent one.

The general architecture observed for all Sm-like proteins is a hexameric or heptameric ring structure. What is responsible for the preference for hexamer or heptamer formation? Since the Sm2 motif is the conserved structure (Table 3), the degree of compaction of the oligomer could be related to some variations in side-chain interactions not involved in the hydrogen-bonding network of the β-sheet. In the Sm-fold responsible for oligomerization, strands $\beta4$ and $\beta5$ lie approximately in the plane and form a β–β corner with an angle of about 50° between them. Such an angle implies that monomers could be packed into heptameric (51.4° per monomer) or hexameric (60° per monomer) ring structures without essential deformation of the Sm2-motif fragment and intersubunit hydrogen bonds. It could be suggested that three hydrogen bonds responsible for elongated β-sheet formation are sufficient to realise a heptameric organization for some proteins of this family, for instance, the AF-Sm1 protein (Törö *et al.*, 2002).

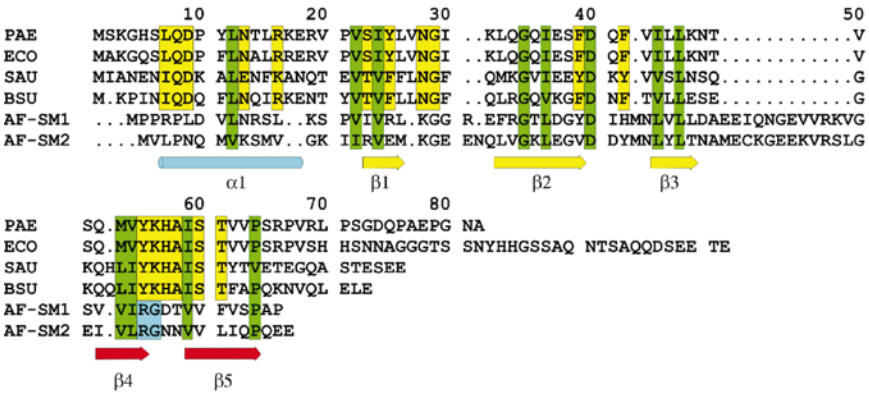

Figure 3
Alignment of Hfq and Sm/Lsm sequences. The number and location of secondary-structure elements correspond to the structure of Hfq from *P. aeruginosa*. The coloured bars indicate the following: yellow, residues conserved among Hfq proteins; green, residues conserved among all presented sequences. Abbreviations: PAE, *P. aeruginosa*; ECO, *E. coli*; SAU, *Staphylococcus aureus*; BSU, *Bacillus subtilis*; AF-SM1, Sm1 protein from *Archaeoglobus fulgidus*; AF-SM2, Sm2 protein from *A. fulgidus*.

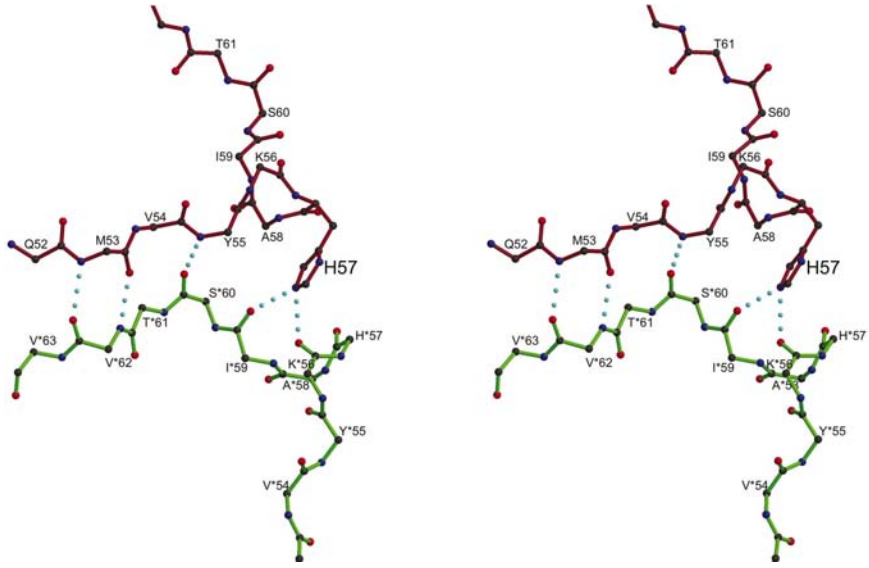

Figure 4
Formation of a hexameric structure of PaeHfq. Backbones of the Sm2 motifs of two adjacent monomers are shown in different colours. Amino-acid residues of neighbouring molecules are marked with asterisks. Hydrogen bonds in the intersubunit interface are shown by dotted lines.

On the other hand, considering the structure and sequence conservation characterizing the Sm-fold in the Hfq family, hexameric organization is a general feature of Hfq proteins (Sauter *et al.*, 2003). In this case the angle of 60° per monomer is realised because the tops of two adjacent monomers are brought together owing to the additional hydrogen bond betweens His57 NE2 and Ile*59 O, which are conserved in all known Hfq protein (Fig. 4). Another conserved hydrogen bond Tyr55 OH–Gln8 OE1 stabilizes the position of helix $\alpha1$ in the hexamer. This helix forms an intermolecular hydrophobic core together with the protein C-terminus and stabilizes the intersubunit interface, making all conserved hydrogen bonds between monomers inaccessible to solvent.

The key role of additional inaccessible hydrogen bonds in hexameric structure formation is also demonstrated by the AF-Sm2 protein (Törö *et al.*, 2002). In this structure, the tops of two adjacent monomers are also brought together owing to the solvent-inaccessible hydrogen bond formed by Asn68 ND2 and Val69 O. It is interesting to note that the substitution Asn68/Thr observed in the AF-Sm1 protein results in the distortion of this additional hydrogen bond and the formation of a heptameric ring structure (Törö *et al.*, 2002). Additionally, cryo-electron micrographs of oligo(U)–AF-Sm2 complexes seem to indicate (Achsel *et al.*, 2001) that assembly of the

protein around a U-rich RNA sequence may lead to the formation of an AF-Sm2 heptamer. Such a rearrangement of the AF-Sm2 ring-like structure could also be explained by the distortion of the above-mentioned hydrogen bond between the C-terminal end of β4 and the N-terminal end of β5.

This work was supported by the Russian Academy of Sciences and the Russian Foundation for Basic Research (grant Nos. 02-04-48536 and 04-04-48556), the Council of the RF President (a grant for outstanding scientific schools No. 1969.2003.4) and the Program for Molecular and Cellular Biology RAS. The research of MG was supported in part by an International Research Scholar's award from the Howard Hughes Medical Institute (grant No. 55000308). The work in UB's laboratory was funded by grant F1715 from the Austrian Science Fund (FWF).

References

Achsel, T., Stark, H. & Lührmann, N. (2001). *Proc. Natl Acad. Sci. USA*, **98**, 3685–3689.
Arluison, V., Folichon, M., Marco, S., Derreumaux, P., Pellegrini, O., Seguin, J., Hajnsdorf, E. & Regnier, P. (2004). *Eur. J. Biochem.* **271**, 1258–1265.
Brünger, A. T., Adams, P. D., Clore, G. M., DeLano, W. L., Gros, P., Grosse-Kunstleve, R. W., Jiang, J.-S., Kuszewski, J., Nilges, M., Pannu, N. S., Read, R. J., Rice, L. M., Simonson, T. & Warren, G. L. (1998). *Acta Cryst.* D**54**, 905–921.
Efimov, A. F. (1992). *FEBS Lett.* **298**, 261–265.
Franze de Fernandez, M. T., Hayward, W. S. & August, J. T. (1972). *J. Biol. Chem.* **247**, 824–831.
Hermann, H., Fabrizio, P., Raker, V. A., Foulaki, K., Hornig, H., Brahms, H. & Luehrmann, R. (1995). *EMBO J.* **14**, 2076–2088.
Jones, T. A., Zhou, J. Y., Cowan, S. W. & Kjeldgaard, M. (1991). *Acta Cryst.* A**47**, 110–119.
Kabsch, W. (1993). *J. Appl. Cryst.* **26**, 795–800.
Kajitani, M., Kato, A., Wada, A., Inokuchi, Y. & Ishihama, A. (1994). *J. Bacteriol.* **176**, 531–534.
Majdalani, N., Hernandez, D. & Gottesman, S. (2002). *Mol. Microbiol.* **46**, 813–826.
Møller, T., Franch, T., Hojrup, P., Keene, D. R., Bachinger, H. P., Brennan, R. G. & Valentin-Hansen, P. (2002). *Mol. Cell.* **9**, 23–30.
Muffler, A., Traulsen, D. D., Fischer, D., Lange, R. & Hengge-Aronis, R. (1997). *J. Bacteriol.* **179**, 297–300.
Navaza, J. (1994). *Acta Cryst.* A**50**, 157–163.
Otwinowski, Z. & Minor, W. (1997). *Methods Enzymol.* **276**, 307–326.
Sauter, C., Basquin, J. & Suck, D. (2003). *Nucleic Acids Res.* **31**, 4091–4098.
Schumacher, M. A., Pearson, R. F., Møller, T., Valentin-Hansen, P. & Brennan, R. G. (2002). *EMBO J.* **21**, 3546–3556.
Seraphin, B. (1995). *EMBO J.* **14**, 2089–2098.
Sledjeski, D. D., Whitman, C. & Zhang, A. (2001). *J. Bacteriol.* **183**, 1997–2005.
Sonnleitner, E., Hagens, S., Rosenau, F., Wilhelm, S., Habel, A., Jäger, K. E. & Bläsi, U. (2003). *Microb. Pathog.* **35**, 217–228.
Sonnleitner, E., Moll, I. & Bläsi, U. (2002). *Microbiology*, **148**, 883–891.
Törö, I., Basquin, J., Teo-Dreher, H. & Suck, D. (2002). *J. Mol. Biol.* **320**, 129–142.
Tsui, H.-C. T., Feng, G. & Winkler, M. E. (1997). *J. Bacteriol.* **179**, 7476–7487.
Večerek, B., Moll, I., Afonyushkin, T., Kaberdin, V. R. & Bläsi, U. (2003). *Mol. Microbiol.* **50**, 897–909.
Zhang, A., Wassarman, K. M., Ortega, J., Steven, A. C. & Storz, G. (2002). *Mol. Cell*, **9**, 11–22.